

Rakesh M. Shedam^a, Priyanka P. Kashid^a, Shridhar N. Mathad^{a*}, Rahul B. Deshmukh^b,
Mahadev R. Shedam^c and Ashok B. Gadkari^d

Ferrites gas sensors: A Review

^{a*}Department of Engineering Physics, K.L.E Institute of Technology, Hubballi – 580027, (KARNATAKA)
India, physicssiddu@gmail.com, physicssiddu@kleit.ac.in;

^bDepartment of Physics, Anna Saheb Dange College Of Engineering And Technology, Ashta-416301, (MS)India;

^cDepartment of Physics, New College, Kolhapur - 416012, (MS) India;

^dDepartment of Physics, GKG College, Kolhapur – 416012, (MS) India

Gas sensors that are highly sensitive, stable, and selective are increasingly in demand to detect toxic gases. As a result of the need to monitor concentrations of these gases, humans, animals, and the environment are all protected. Metal ferrites (AFe_2O_3 , where A is a metal) are a major factor in this field. The development of ferrite gas sensors has made remarkable advances in the detection of toxic gases from vehicle exhaust, biological hazards, environmental monitoring, and pollution monitoring over the last decade. It is important for ferrite gas sensors to consider parameters like phase formation, crystallite size, particle size, grain size, dopants, surface area, sensitivity, selectivity, operating temperature, gas concentration, response time, and recovery time. There are various materials for gas sensing use such as carbon monoxide (CO), carbon dioxide (CO₂), methane (CH₄), ethyl alcohol (C₂H₅OH), hydrogen sulfide (H₂S), C₂H₅COOH, oxygen (O₂), hydrogen (H₂), chlorine (Cl₂), NH₃, C₄H₁₀, CH₃COOH, gasoline, acetylene, petrol, and liquefied petroleum gas (LPG). Various methods are used to prepare ferrite gas sensors. Additionally, a brief description is provided of the various methods employed for synthesizing ferrite gas sensors. A comprehensive survey of ferrites as gas sensors, such as nickel, copper, zinc, cadmium, cobalt, magnesium, manganese, and multi-component ferrites, prepared by various methods.

Keywords: Gas sensors, Ferrites Thick films.

Received 22 June 2022; Accepted 19 September 2022.

Introduction

Different chemical substances are present in the air that we breathe, some of them useful, others dangerous. Gas pollutants that are toxic and harmful have become an issue of concern in recent years [1]. As a result, gas detection and monitoring has become increasingly important. Gas sensors should fulfill two essential functions: the receptor and the transducer. A sensor's first function is to recognize a particular gas species (via adsorption, chemical or electrochemical reactions) and its second function is to translate that recognition into a sensing signal (e.g. resistance change, capacitance, electromotive force, resonant frequency, optical absorption or emission). There are also work function, mass, optical characteristics, gas/solid interactions, and

magnetic interactions (magneto-optical Kerr effect), among other things. Generally, gas sensors are designed to enhance two functions [2, 3], i.e. increase the receptor function, which is normally related to selectivity, and increase the transducer function, which is related to sensitivity. To accomplish the two functions, there are different sensing techniques, which result in different sensor techniques, which include electrochemical gas sensors [4-5], optical gas sensors [6], thermal conductivity gas sensors [7] and acoustic gas sensors [8,9]. Monitoring and measuring the concentrations of useful gases are also necessary in industry for the manufacture of a wide variety of products. The gases to be monitored in industry and healthy environments are NO₂, CO₂, H₂S, NH₃, and Cl₂. Current research activity is focused on the issue of monitoring these gases. They will be used in monitoring

stations for the environment [5]. Thin film, pellets, and films of thick films are used in the fabrication of the sensors [10,11]. Gas sensors are constructed to perform the a forementioned two main functions, durable as well. Researcher have focused on developing new materials to achieve highly sensitive and selective long term operating device for gas sensor but most have less than selectivity (distinction between one gas and other interfering gases). Most of the reducing gases can be defected using tin dioxide [12,13]. The main disadvantage is that it has low sensitivity. Several new materials can be investigated with extraordinary gas sensing abilities. As gas sensors, ferromagnetic material have become popular because they higher selectively and stability for particular gas than n type semiconducting oxides many studies have been carried out on ferrite material and how to prepare ferrite gas sensors [14-21]. In an article published by primz et al. [20] they reviewed magnetic materials essential for information storage in electronics. According to wang et al [21] MFeO(MCo-ni) ribbons prepared by the gel technology exhibit very low saturation magnetization and coercivity at room temperature. Teases properties increases low temperature cobalt ferrite ribbons. When a cobalt ferrite ribbon is subjected to low temperatures, saturation magnetization and coercivity increase. The ribbons can be used in gas sensors and electronic devices. Ferrites have become increasingly important to sensor technology and other electronic applications over the past decade. First attempt has been made to use nickel ferrite (NiFeO) as a sensor for the rapid detection of chlorine gas [22]. The high density of ferrites has also been studied extensively [23- 25], as well as their catalytic [26], magnetic, and electrical uses [27-29]. The nickel ferrite gas sensor was reported by Arai and Seiyama [30]. Cadmium ferrite, a semiconducting material, has been used for high-performance ethanol sensors [31]. Gopal Reddy et al. [33] explore zinc, copper, nickel, and cobalt ferrite as potential detectors. Toxic gases and chlorine. As important mixed oxides for gas sensors, Chen et al. [34] studied spinel-type oxides with formula MFe₂O₄ (M= Cu, Zn, Cd and Mg). Both oxidizing and reducing gases could be detected with these oxides. In a study by Shimiza et al. [35], magnesium, zinc, nickel ferrite was compared with chromites such as magnesium, zinc, and nickel in terms of their ability to detect oxygen. Researchers observed more oxygen sensitivity in p-type chromite than in n-type ferrite. According to Liu et al. [36], the n-type semiconductor CdFe₂O₄ exhibits high sensitivity and selectivity for alcohol vapors. Researchers have studied gas sensors with small particles and large surface areas in the last decade [37-38]. Recent research has shown that ferrites can be used for gas sensing applications [34,39-41].

For the production of ferrite gas sensors, several techniques have been studied. As examples of these, solid state method [42], decomposition [43], chemical precipitation [44,45], sol-gel [46], self-combustion [47], citrate [33,34], co-precipitation [24, 25, 48, 49]. The preparation of multi component oxides is considerably easier and more effective when done using co-precipitation [49]. In this communication, we present a comprehensive review of ferrite gas sensors and their characteristics.

I. Parameters of gas sensing

In this article, we examine the parameters that are crucial in gas sensing, and especially to the use of ferrites as sensors. Various metal ferrites are used as different gas sensors. Table 1 summarizes the optimized parameters of gases.

2.1. Pore structure

There are three kinds of pores found in ceramics: open passage pores, closed pores, and internal pores [50]. There are numerous shapes of porous structures depending on the cross section of the cross section. Pores can be classified as microspores (about 2 mm), mesoporous (between 2 and 200 nm), or macrospores (typically 200 nm in diameter). The porosity ratio is the proportion of pore volume to total pores.

$$P = \frac{V_p}{V}, \quad (1)$$

where V_p the total is pores volume and V is the volume of the body.

As the adsorption of gas analytes takes place at the surfaces of porous sensors, porosity influences sensitivity[51]. Ferrites with open pores exhibit improved sensitivity. CO_{1-x}Ni_xFe₂O₄ [52] sensor has high porosity, reducing its sensitivity to CO and ethanol. The sensitivity of the LaFe₂O₄ LPG sensor [53] is influenced by the large number of pores.

The open pores enable for faster adsorption of the test gas analyte, resulting in a quicker reaction. It has been observed that porous CuFe₂O₄ has superior gas sensing characteristics toward acetone [54].

This was attributed to the porous nanostructure and, secondarily, the CuFe₂O₄ nanospheres surface. Recent research on ferrites nano-particles [55], nanorods [56], [57] nanospheres [58] nanocubes [59] nanoparticulate thin films [60], and [62] nanoplates [62] all concur that larger porosity in gas sensing is beneficial.

B. Sensor Resistance to Gas Concentration

The effect of gas concentration (C_g) on sensor resistance (R_S) or conductivity (G_S) is explained by this characteristic. In an atmosphere with low concentrations of gas, at a constant temperature, the conductivity (G_S) would be [61],

$$G_S = KC_g^\alpha, \quad (2)$$

Where K and α are constants, and stands for gas concentration parameter in air.

C. Sensitivity

Defining sensitivity as the ratio in Eq.(2) [62] where R_g indicates sensor resistance in the presence of test

A gas analyte is present, and R_a is the resistance of the sensor.

$$S = \frac{R_a}{R_g} \text{ sensitivity for reducing gas or}$$

$$S = \frac{R_g}{R_a} \text{ for oxidizing gas} \quad (3)$$

The resistance change in test gas analyte (and air) can also be referred to as the resistance ratio, Eq. (6).

$$S(\%) = \frac{(R_{\alpha} - R_g)}{R_g} \times 100, \quad (4)$$

Concentration of gas (usually a direct relationship)[63,64] as well as type of ferrite determine it.[65,66] The sensor resistance increases for an oxidizing gas analyte, but breaks down for a reducing gas analyte. Porosity, pore size, and the specific area can also affect the sensitivity. Within certain limits, surfaces with large specific areas are usually highly sensitive. The control of these parameters is one of the most challenging aspects of ferrite sensor fabrication. A suitable sintering temperature and the introduction of additives that stimulate pore formation to solve these problems. Gas sensitivity reaches saturation at high concentrations [67]. Patil et al. As the concentration was increased stepwise from 5-60 ppm, α -Fe₂O₄ sensitivity to LPG increased. The sensitivity of a ZnFe₂O₄ LPG sensor increased with increasing concentrations, as shown by Rezliescu et al.[68]. Depletion layer width affects the sensitivity of semiconductor ferrites [69].

Selectivity

Sensors are selective when it comes to responding to certain gases in the presence of other gases. Operating temperature is closely related to this [70]. Gases with varying chemical compositions can be superimposed and result in sensor reactions that are a sum of their respective effects. Adsorption of gas molecules on the surface of grains is the process by which gases are detected. Chemical reactions occur on the surface as a result of adsorption. In order for the chemical reaction to work effectively, the sensor must be heated to a higher temperature. Four different methods are employed to enhance sensitivity and selectivity [70,71].

- 1) temperature control;
- 2) use of catalyst and dopants;
- 3) special additive to the grain surface;
- 4) use of filters.

By using the right electrode configuration and thickness of the sensing layer, selectivity can also be improved. Geometrical properties of electrodes, including their location and distance from the sensing element layer also affect the relative measure of sensitivity and selectivity [70].

Operating Temperature

Ceramic gas sensors are sensitive to changes in operating temperature, one of many factors that determine the sensitivity. Resistance changes in reaction with presence of a given gas are dependent on activation processes, such as the reaction speed on the grain surface and the diffusion speed of the gas molecules. Chemical reactions are limited by the speed of reaction at low temperatures, and the diffusion of gas molecules is limited by the speed of diffusion at high temperatures. When the temperature is this high, the response is maximal. The response is greatest at this temperature. For every gas, a specific temperature is required to achieve its maximum sensitivity. Several factors determine the temperature in

which peak values occur, including gas composition, chemical composition, additives, and catalysts [61].

When the temperature increases, most of the sensors present an increase-maximum-decay trend for various gases. Metal-oxide semiconductor sensors display their sensitivity according to the interaction between the target gas and the sensor surface. The gas molecules cannot react with the surface adsorbed O at low temperatures because they lack sufficient thermal energy. This leads to a very low rate of reaction between the targeted gas and Oxygen. Therefore, the sensitivity is low. As the temperature is raised, the increase in sensitivity can be attributed to two factors: 1) sufficient thermal energy to overcome the activation energy barrier of the surface reaction and 2) much higher electron concentrations in the target gas as the oxygen species are converted to oxygen at higher temperatures via the sensing reaction. At higher temperatures, exothermic gas adsorption becomes more difficult, resulting in a reduction in sensitivity after the maximum. A high sensitivity can be obtained by considering an optimal temperature [73,74].

Response Characteristics

In response to a change in gas concentration, response characteristics are determined by the time resistance. The transition from clean air to a gaseous atmosphere is established by establishing a defined temperature and gas concentration, and the response is then measured [61]. Rise time and fall time are considered, when evaluating response characteristics. Detection of gas takes place after a sensor's rise time has passed. After the test gas has been removed, the fall time indicates the length of time it will take for the value to return to its original value [19,22].

Crystallite Size, Grain Size/Particle Size

Each crystal within a grain or particle is called a crystallite. Every grain contains several crystals. A grain's diameter is in addition to its particle size. When the particle size is less than about a 10⁻⁵ centimeter (1000 Å), it is referred to as grain size decreases, strength and hardness will increase [74]. In their study of copper, zinc, cadmium, and magnesium ferrites, Chen et al. [34] investigated the effect of grain size. The surface area (grain size) was found to affect the gas sensitivity. Gas sensitivities are higher in smaller grain size samples (larger surface area) than in larger grain size samples (smaller surface area). The most efficient way to increase the sensitivity of the sensor would be to increase the surface area of the material.

Surface State

The surface state determines gas sensing at low concentrations [75,76]. Localized energy levels on the surface of a material determine the surface state. It is possible to identify intrinsic and extrinsic surface states in ionic crystal materials. The intrinsic surface states are determined by the lattice distortion periodicity at the surface of the material. The extrinsic states, on the other hand, arise when gases and impurities bind to a surface.

Additives/Dopants

Ferrite gas sensors are commonly tuned by adding rare earths and metal ions to them in order to improve

sensitivity, selectivity, and response time. In a study by Muraishi et al. [77], they evaluated the effect of rare earth oxide additives on nickel ferrite sensors. They found that the additives La₂O₃, Sm₂O₃, and Y₂O₃ improved the sensor's sensitivity and shortened its response time significantly. Satayanayana et al. [78] Examined the effect of Co, Mn, and Pd on the nocrystalline structure of nickel ferrite. Incorporating 1 wt% of Pd into the LPG sensor, we observed improved sensitivity, selectivity, and response times, as well as a reduced operating temperature [79]. Reddy et al. [80] found that palladium incorporated into nickel ferrite reduced the temperature of operation and accelerated the response time. A temperature-dependent sensitivity study of manganese substitution in Ni–Co ferrite was published by Iftimie et al. [47]. Researchers Izabela et al. [81] examined manganese substituted cobalt ferrite. Zhang et al. [48] studied the properties of Pt, Pd, Ce, Mg, Sr, La, and Bi for nanozinc ferrite. Using Ce and La adulterated zinc ferrite, they found good sensitivity and selectivity. Rezelescu et al. [82] reported Mg-Cu ferrite with La, Ga, and Y substitutes. Ga containing ferrite was found to be most sensitive to changes in humidity.

Phase Formation

Ceramic materials can exist in different phases, depending on their composition and temperature. Gas sensors based on solid-state ceramics containing rare earth orthoferrite as an auxiliary phase have great potential for gas detection. The response time of these materials was fast when the sensor was used as an auxiliary phase. Electrochemical stability is improved by perovskite-type oxides as auxiliary phases Performance of sensors [83]. In orthoferrites, there can be phases such as Y³⁺Fe₂O₄, Gd³⁺Fe₂O₄, Sm³⁺ Fe₂O₄, La³⁺Fe₂O₄, and Nd³⁺Fe₂O₄ [84,85-88]. If the ferrite contains more than one phase, its properties depend on those of each phase separately and the way they occur in the aggregate. In general, such materials offer a wide range of structural possibilities because they can have grains of different sizes and orientations than other phases [74].

Surface Phenomena and Gas Sensing Mechanism

1) Adsorption: The absorption of atoms, molecules, or ions into a solid, liquid, or gaseous phase is a physical or chemical phenomenon. By spreading out into the volume, molecules dissolve into liquid or solid, becoming a solution. A solid will fill its pores this way [89]. An adsorbate is formed when molecules or atoms are accumulated on the surface of an adsorbent (adsorbent), resulting in the accumulation of gas or liquid solute. A body's surface is used to capture atoms or molecules. That's how it captures atoms and molecules. The binding of particles or molecules to the surface. Such a connection tends to be strong but temporary. Adsorption and absorption are both sometimes referred to as sorption [61,90].

Physical and chemical adsorption are two types of adsorption [48]. By electrostatic interaction with the surface, atoms or molecules can retain their individuality in physisorption (physical adsorption). There is no more than 0.1 eV of energy required to bind to the surface in this case. Adsorption and desorption at low temperatures are caused by these phenomena. When an atom or molecule is

adsorption, its electronic structure is barely perturbed [91,92]. In physisorption, the Vander Waals force exerts an interacting force, based on the mutually induced dipole moments of molecules or atoms that produce Van der Waals forces.

In chemical adsorption, molecules or atoms are chemically linked with the crystal. They are mostly covalently and partly ionically bonded. If the energy is over 1 eV, binding chemisorption occurs at high temperatures [61]. An adsorbent-adsorbate interface characterized by high electron density, strong interactions between the adsorbate and a substrate surface, and high temperature is characteristic of chemisorption [89-91]. A multilayer adsorption of gas phase molecules can occur under appropriate conditions for physisorption. Chemical adsorption occurs when molecules form monolayers on surfaces by virtue of their valence bonds. Whatever the type of adsorption, the adsorbed molecules or atoms form donor or acceptor levels on the surface.

Adsorption and absorption involve sorption (adsorption and desorption) [90]. An equilibrium state of sorption occurs when there is an adsorption surface (solid or boundary separating two fluids) and a bulk phase (fluid, gas, or solution). Some of the sorbed substance changes to a bulk phase when the concentration of a bulk phase is lowered. As one component of a liquid stream transfers to the vapor phase by mass transfer through an interface between liquid and vapor, stripping is also known as desorption [89].

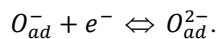
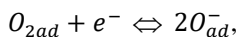
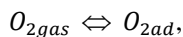
2) Surface States: Surface energy levels at the surface of materials are localized state energy levels. Solid material ends abruptly with a surface, leading to these states. They can only be found on atom layers near the surface. An electronic bond structure changes from a bulk material to a vacuum as a result of a surface on the termination material. There are two kinds of ionic crystal states in semiconducting metal oxide, for example [70].

Surface intrinsic states are generated by distortion of the lattice periodicity at the surface. Tamm [93] determined the intrinsic energy of localized electronic states based on the termination of periodicity in crystal lattices. When the electron affinity of surface species and bulk species differ substantially, a Tamm state may be induced for an ionic crystal. Transition metals and wide-gap semiconductors can be described by Tamm states [90, 94]. For covalent materials, Shockley defined intrinsic surface states in which the atom at the surface forms dangling bonds [70]. The nearly free electron approximation is used for calculating the states of clean and ideal surfaces. Normal metals and some narrow gap semiconductors can be described using this approach [90,95].

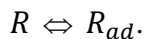
A clean, well-ordered surface is usually not the source of intrinsic states. Gases and impurities are absorbed by the surface, leading to the formation of these particles. Including defect surfaces as well as adsorbate and liquid-solid interfaces between two materials, such as semiconductor-oxide and semiconductor-metal. There may also be extrinsic states if there is a defect at the surface interface between two materials, such as a semiconductor-oxide or semiconductor-metal interface between liquid and solid phases [70,95,96].

Gas Sensing Mechanism: Oxides like Cl₂, CH₄, CO,

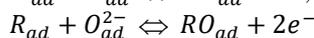
and ethanol create a change in resistance thanks to reducing gases. An electron is extracted from the bulk of oxygen adsorbing on the surface of the sensor, which ionizes into O^- or O^{2-} (O is more prevalent at $100^\circ C-500^\circ C$, so the resistance is lower). A reducing gas, such as CO , reacts with the adsorbed O , releasing a trapped electron to the conduction band and resulting in a reduction in resistance. This conductive gas sensor is believed to sense the ambient gas concentration through a change in resistance proportional to the amount of reducing gas present [70]. To understand the fundamental process behind gas sensors, understanding how gases interact with oxide is important. Adsorption of gases causes a change in resistance or capacitance in sensors. Gas sensors conduct due to oxygen-related chemi-adsorbed species, including OH^- , O_{2ad}^- , and O_{ad}^{2-} [17,97]. It relies on surface-controlled processes to sense gas in ferrite. Generally, it is possible to describe surface-controlled processes for oxide semiconductor gas sensing materials as follows [98,99]. Oxygen can be adsorbed and ionized from air containing the test gases as follows:



Where "gas" denotes gaseous oxygen, while "ad" indicates oxygen adsorbed on gaseous oxygen. Depending on the sensor materials, the reducing gases (R) may be absorbed as [100, 101].



The reaction between the adsorbed gas and adsorbed oxygen species is for example, O_{ad}^- and O_{ad}^{2-} which will then proceed as follows:



Finally, desorption of the resulting product will take place as [101]



Sensor materials and test gas type influence gas adsorption, which affects sensor sensitivity and response time. The large amount of gas that is absorbed and the easy reaction between the adsorbed reducing gases and oxygen species indicate high sensitivity [99]. Different gases have different gas sensing properties due to differences in the adsorption and reaction processes. Providing enough reactants for reactions depends on the amount of adsorbed oxygen species [102]. It is however possible to enhance gas sensing by adding some catalytically active compounds [11].

Fabrication of Gas Sensors:

Sensors can be made of large-grained or nanocrystalline materials and can be made in pellets, thick films, thin films, or a combination of both, utilizing a variety of techniques, such as: 1) a conventional sintering process for the bulk pellet type; 2) a screen printing

process for thick films; and 3) a vacuum deposition process for thin films. Materials such as these are promising because they can be fabricated reproducibly, are relatively inexpensive, and have faster gas responsiveness

1) Bulk Type: Conventional ceramic sintering produces rectangular and cylindrical shapes in most commercially available products. The ferrite sensors operate at temperatures between $300^\circ C$ and $500^\circ C$. Due to their structural properties, ferrite sensors are highly stable, therefore, they can be used to detect reducing, toxic, and inflammable gases [40,103,104].

2) Thick Film Type: For screen-printed thick-film sensors, the size of the sensor can shrink to about $1\text{ mm} \times 1\text{ mm}$ and hence, low power consumption can be achieved. In order to prepare the paste, chemically sensitive powder is mixed with an organic binder, such as Polyvinyl alcohol. Coatings are applied to alumina and ceramic tubes [12,13,22,33, 105-107].

3) Thin Film Type: It is important to use thin film sensors because of their higher performance and ability to integrate into devices. There are several different methods of deposition that can be used to obtain low-power devices on conventional silicon wafer substrates, including evaporation, sputtering, and spary pyrolysis [33,108,109].

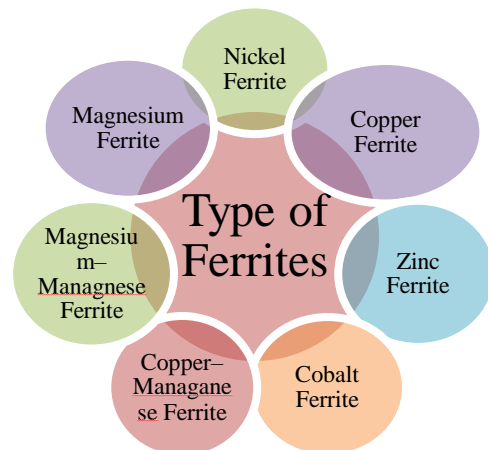


Fig.1. Various types of ferrites.

Nickel ferrite:

In their article, Reddy et al. [17] characterized nanocrystalline nickel ferrites using microemulsions and hydrothermal methods. As compared with the micelle technique, nickel ferrite prepared by the hydrothermal method has high sensitivity at low temperatures. The response time for ferrite synthesized by the micelle technique is faster ($\sim 10s$) than that of the hydrothermally synthesized method ($\sim 1\text{ min}$).

According to Gopal Reddy et al. [33], the low level of chlorine gas could be detected by using virgin nickel ferrite (p-type). A single phase is formed at $600^\circ C$ and the sensor was prepared by the citrate method. A high degree of sensitivity to chlorine was found at operating temperatures between $250^\circ C$ and $300^\circ C$. All other test gases (LPG, H_2S , CO_2 , CH_3) exhibited a very low sensitivity when compared to chlorine. Researchers found that metal added to the material improved sensitivity and reduced response time. Muraishi et al. [39] studied the sensing characteristics of porous nickel ferrite added with rare earth metal oxide. The addition of rare earth metal oxides led to an increase in sensitivity to saturated

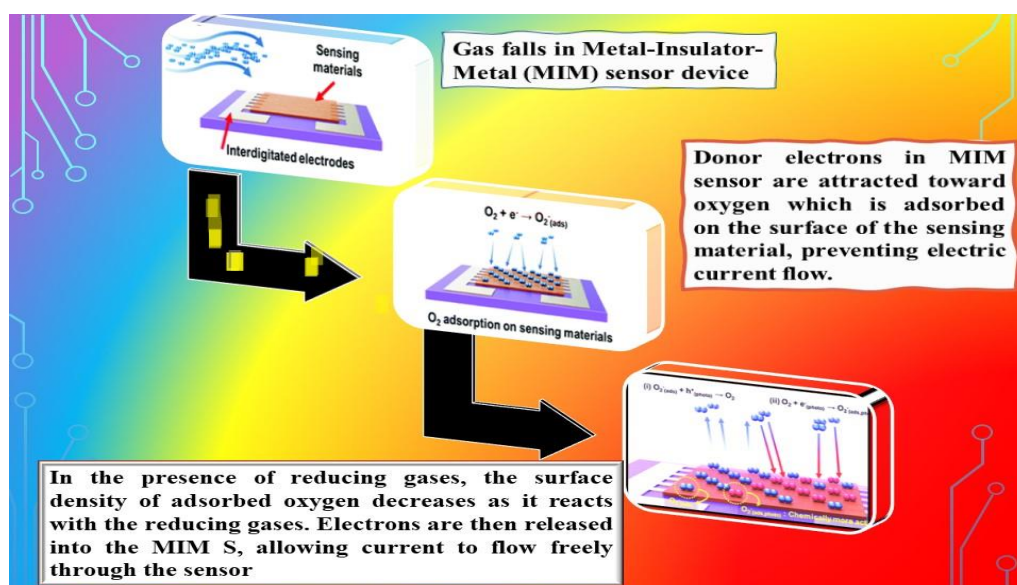


Fig.2. Schematic diagram of the oxygen adsorption process [101].

hydrocarbon gases and a more rapid response time.

Iftimie et al. [47] used metal nitrate and ammonium hydroxide as raw materials to prepare polycrystalline nickel ferrite doped with cobalt and manganese. Acetone, ethanol, methane, and LPG were examined for their sensing properties. A bulk density of 3.11 g cm³ was determined. It is noted that the sample shows maximum sensitivity to acetone at 230 C and then decreases in the range of 125 C-285 C thereafter. It is found that the operating temperature of LPG is reduced between 210 C and 230 C. The mechanism used to accomplish this is thermally activated [78].

In their study, Satyanarayana et al. [78] prepared nanosized Nickel ferrite doped with cobalt and manganese using the hydrazine method. This ferrite was studied for gas sensitivity to LPG, CO, and CH₄. It is found that sensitivity depends on the composition, crystallite size, surface area, and gas to be detected. Maximum sensitivity to LPG is observed at 230 C. Due to the change in composition of ferrite, the operating temperature is reduced from 230 C to 210 C. Palladium increases selectivity, sensitivity, and response time while decreasing the operating temperature from 230 C to 180 C.

Darshaneet al. [77] A low temperature, less expensive, and environment-friendly method used to synthesize NiFe₂O₄ nano-powder has been described. With higher processing temperatures, sodium chloride inhibits grain growth naturally. A NiFe₂O₄ nanomaterial-based sensor shows selective response towards 200 ppm of LPG with a response time of a few seconds and good reproducibility at 400°C.

Copper Ferrite:

A copper ferrite was prepared in a citrate method by Gopal Reddy et al. [33]. At 900 C, the single phase sensor elements were sintered at 600 °C for 2 h. A variety of gases were tested, such as LPG, H₂S, CO₂, Cl₂, CH₄, etc. ferrite (p-type semiconducting oxide) exhibits high sensitivity to reducing gases, namely hydrogen, carbon dioxide, and liquefied petroleum gas at 150-350 degrees Celsius. A sensitivity of about 0.4 is observed for these

gases. The size of the crystallites and their specific surface area are 29.39 nm and 8 m²/g, respectively.

According to Chen et al. [34], copper ferrite was prepared by co-precipitation method and characterized for its gas sensing properties, such as CO₂, H₂, LPG, C₂H₅OH, and C₂H₆. The sample shows a spinel structure due to its single phase structure. At 250 C, this ferrite shows sensitivity to alcohol vapor, LPG, and C₂H₂, but is less sensitive to CO₂ and H₂.

Rezlescu et al. [104] reported copper ferrite sintered at 1000 °C using the sol-gel self combustion method. We tested the sensor for LPG, C₂H₅OH, and CH₃COOH₃. Using 350°C as the operating temperature, it shows sensitivity to LPG. Granules are approximately 700 nm in size and 24 mg in surface area. A sensor responds in three minutes, and it recovers in four minutes. Sun et al. [111] reported that copper ferrite could be synthesized by solid-state reactions. Copper ferrite sensors were tested against reducing gases, ammonia, acetone, hydrogen, and ethanol gases. Different operating temperatures cause variation in response for different gases.

Zinc Ferrite:

Arshah et al. [106] investigated the effects of NiO/TiO additions on zinc ferrite gas sensors. Screen-printed thick films were tested for ethanol, propanol, pentanol, butanol, and hexanol. Hexanol was the most sensitive solvent. Incorporating TiO/NiO improved the response and recovery time. With increasing sensor temperature, response and recovery times decrease. Citrate zinc ferrite prepared by Gopal Reddy et al. [22] was reported to be an n-type oxide. The sensor elements were sintered at 600°C for 2 h and tested for gases such as LPG, H₂S, CO₂, Cl₂, CH₃, etc. Hydrogen sulfide exhibited the highest sensitivity. At a temperature of 325 C, the sensor is most sensitive to LPG, but responds poorly to other gases.

Darshane et al. [41] synthesized zinc ferrite via molten-salt incorporation of sodium chloride as a growth inhibitor. As a result of sintering at 700°C, a single-phase cubic structure formed. At an operating temperature of

250°C, the zinc ferrite has greater sensitivity and selectivity for H₂S compared to Zn-doped ferrite synthesized by other routes. A response time of 30 seconds and a recovery time of 3 minutes can be expected. Nanosized particles are responsible for the low response time.

Jiao et al. [48] developed a co-precipitation method for the fabrication of nano-zinc ferrite gas sensors. 650°C was used to calcine the ferrite mixture for 6 hours. A spinel structure was observed on XRD. Crystals are approximately 30 nm in size. The sensor shows better sensitivity to Ce and La adulterants. A slight increase in sensitivity to acetic acid gas is caused by the Pt, Pd, Mg, Sr, and Bi adulterants. When adulterated with Ce, the sensor is most sensitive to acetic acid gas. It isn't sensitive to organic gases such as ethanol or acetone. The correlation between sensitivity and concentration is also found to be good. As a result of gas-solid interaction, the gas sensing phenomena is a surface effect, which means the larger the surface area, the greater the sensitivity. Due to its small grain size (less than 30 nm) and larger surface area, the zinc ferrite gas sensor is highly sensitive to C₂H₅COOH.

Cadmium Ferrite

According to Tianshu et al. [17], cadmium ferrite can be prepared by the co-precipitation method and can be tested for C₂H₅OH, CO₂, H₂, and C₄H₁₀. CdFe₂O₄ consists of grains whose sizes range between 50 and 150 nm. At a temperature of 380°C (90 at 200 ppm), the sensor exhibits high sensitivity and rapid response. It can detect ethanol vapors as low as several parts per million. Sensors of this type may be used to test breath alcohol levels.

Co-precipitated cadmium ferrite [34] shows greater sensitivity to acetylene at operating temperatures of 250°C. The material is insensitive to hydrogen and carbon monoxide gas. There are 33 nm grain size and 80 m²/g specific surface area. In addition, they found that sensitivity to gases depends on the kind of ferrite and the specific surface area.

Using the sol-gel self-combustion method [104], cubic spinel cadmium ferrite was prepared and tested for gases such as LPG, C₂H₅OH, and CH₃COCH₃. When operating at 350°C, it is less sensitive to LPG than alcohol and acetone. There are about 300 nm of grains and 6 m²/g grains of surface area in the cadmium ferrite prepared by Lou et al. [112] using the sol gel method. For samples sintered at 700°C, the results showed high sensitivity and selectivity. A sensor at an operating temperature of 250°C responded with a reading of 55 at 100 ppm.

Cobalt Ferrite

Gopal Reddy et al. [33] report a citrate method for preparing cobalt ferrite. Hydrogen sulfide (~0.6) is the most sensitive gas to this p-type semiconducting oxide at temperatures of 225°C–250°C. Chlorine gas sensitivity increases with increasing temperature and increases up to 400°C. According to the report, the crystallite has a size of 18.07 nm and has a mass of 11 mg.

Magnesium Ferrite

According to Rezlescu et al. [19], magnesium ferrite is prepared by autocombustion using metal nitrate and Sn

and Mo ions. Sn containing MgFe₂O₄ exhibited the finest granulation of 100 nm. Several reducing gases such as ethanol and acetone were tested for the gas sensing properties. Almost all ferrites are more sensitive to acetone than ethanol. Depending on the type of substitution and test gas, the sensitivity will vary.

Darshane et al. [113] studied the effect of Pd on the gas sensing properties of magnesium ferrite. Sensor element responds to LPG at 200 ppm, as does Pd-doped magnesium ferrite. Operating temperature is lowered from 350 C to 200 C for Pd-doped magnesium ferrite. With the oxalate co-precipitation method, we synthesized semiconducting n-type magnesium ferrites. A cubic spinel structure was confirmed by XRD. There was a reduction in grain size and crystallite size. LPG, CHOH, and Cl₂ were tested with the magnesium ferrite sensor. The sensor shows the greatest response to LPG. We observed the maximum response to be 63% at 800 ppm at room temperature. The solid-state synthesis of magnesium ferrite nano particles n-type by Liu et al. [114] was achieved by a solid-state reaction. The magnesium ferrite sensor showed the highest response to LPG. CH₄, H₂S, and C₂H₅OH were also tested.

The self combustion method was used to prepare magnesium ferrites with substitutions of Sn⁴⁺ and Mo⁶⁺ [115]. Gas sensing responses to acetone and ethanol were studied using sensor elements. Samples with Sn substitution have the highest porosity and specific areas of 24 m²/g. Samples with Sn substitution have a higher sensitivity than pure magnesium ferrite. During the gas sensing study, it was found that sensitivity depends on temperature, particle size, and composition. MgFe₂O₄ with Sn doping is more sensitive than MgFe₂O₄ with Mo⁶⁺ substitution. The higher porosity and nanoparticles of MgFe₂O₄ substituted with Sn contribute to the faster response.

Conclusion

From the literature, co-precipitation has been found to be a very effective method to prepare a broad range of gas sensors as preparation technique, sintering temperature, gas concentration, and response time affect sensitivity, selectivity, and response time. By using the co-precipitation method, nickel ferrite is prepared with a good response to chlorine and acetone. Compared to zinc ferrite, magnesium ferrite and cadmium ferrite are sensitive to ethanol and LPG, respectively. Doped ferrites are also found to have a higher sensitivity than undoped ones. Adding dopants to ferrites reduces reaction time and operating temperature. To achieve sensitive and selective long-term devices, new materials are needed for the gas sensor. Ferrites will certainly be used as gas sensors in the future due to the continuous development of technology. Researchers' innovative research will drive the increasing demand for developing ferrite gas sensors for industrial products, processes, and other applications.

Ferrites gas sensors: A Review

	Ferrites	Synthesized methods	Sintering Temperature (in °C)	Operating	Sensitivity	Selectivity	Concentration (ppm)	Crystalite size (Å nm)	Particle size (nm)	Response time	Recovery Calcination Operating time	References
1.	ZnFe ₂ O ₄	solid-state chemical reaction.		260 °C , 300 °C.		Methanol ethanol	100	-	30 nm	37.3 29.1	5s 26s	116
2.	CdFe ₂ O ₄	Sol-gel self-auto-combustion	1000°C	350° C		LPG, C ₂ H ₅ OH and acetone	150	300		200–250 s	250–300 s	117
3.	NiFe ₂ O ₄ + rarer earth	ceramic	1100-1250 °C	1100°C	Max	Sachurated hydrocarbon	-	17.5	-	-	-	33
4.	NiFe ₂ O ₄ + Co-Mn	Sol-gel self-auto-combustion	1273 °C	488°C	Max	CH ₃ COCH ₃	1000	-	0.1µm	180	330	118
5.	NiFe ₂ O ₄ + Mn ⁺ Co(poly)	Self Combustion	1000 °C	125-285°C	4.5	CH ₃ COCH ₃		100-500	0.1µm	-	-	47
6.	Co _{0.01} Mn _{0.02} Fe _{1.98} O ₄	Self-combustion	1000 °C	230 °C	--	C ₂ H ₅ OH, CH ₄ , LPG		100–500	0.1 mm	-	-	119
7.	Co _{1-x} Mn _x Fe ₂ O ₄	Chemical spray pyrolysis	900 °C	150°C	90%	NO ₂	100	45–65		1.62	-	120
8.	CoFe ₂ O ₄	wet chemical	175 °C	227 °C		NH ₃	25	40	--	--	--	121
9.	CuFe ₂ O ₄	Sol-gel auto-combustion	700°C	80 °C		H ₂ S	25	32	35.8±65.3 s	51.5±63.4 s	--	122
10.	CuFe ₂ O ₄	Sol-gel self-auto combustion	1000 °C	350°C	90%	C ₂ H ₅ OH, acetone and LPG	150	700		3 min	4min	123
11.	CuFe ₂ O ₄	Auto-combustion	600 °C and 900 °C	300 °C		ammonia (NH ₃), Acetone(CH ₃ COCH ₃), hydrogen (H ₂) and ethanol gas (C ₂ H ₅ OH).	1000	60-80	40–60			124
12.	Li _{0.5} Sm _x Fe _{2.5-x} O ₄	Sol-gel self-auto-combustion	850°C	60°C	80–87%	Methanol and C ₂ H ₅ OH LPG and NH ₃	200	100–200		≈3min	≈5–6 min	64
13.	Li-CuFe ₂ O ₄	Co-precipitation	900 °C	340–355 °C	83.82%	LPG	50	≈23	≈58	32 s	2–3 min	125
14.	MgFe ₂ O ₄	Sol-gel auto combustion	1173 K	250 °C	71%	LPG	200		30–38			126
15.	MgFe ₂ O ₄	Co-precipitation	900 °C	335 °C	3.0	Petrol	5	40	1mm			127
16.	MgFe ₂ O ₄	Solid state reaction	700 °C	275 °C		C ₂ H ₅ OH	10–1000		15–30			128
17.	MgFe _{2-x} Ce _x O ₄	Sol-gel auto combustion	973K and 1173 K	25 °C	94%	Acetone	100–300	28–34	0.07–0.2 µm	20 s	65 s	129
18.	MgFe ₂ O ₄ +Sn ⁺⁴ and Mn ⁺¹	Auto combustion			Max	CH ₃ COCH ₃			100			19
19.	MgFe ₂ O ₄	Co-precipitation	400°C	250°C	Max	LPG	2000		32			34
20.	MgFe ₂ O ₄ +Pb	Molten salt	400°C	200°C	370	LPG	200	15-20	8-15	3	120	113
21.	MnFe ₂ O ₄	Solution assisted combustion		300 K	80.6%	SO ₂		10.7		1 s	5 min	130
22.	ZnFe ₂ O ₄	Sol-gel self-auto combustion	1000 °C	350°C	90%	C ₂ H ₅ OH, LPG and acetone	150	100		2 min	4 min	131
23.	ZnFe ₂ O ₄	Sol-gel self-auto combustion	500°C	25 °C	140%	LPG	2000	10	30–40	60 s	300 s	132
24.	ZnFe ₂ O ₄	Ultrasonic spray pyrolysis		280 °C	10	CO	500		10	70 s	90 s	133
25.	Ag-NiFe ₂ O ₄	Solid state		800 °C	43	Acetone				1 s	≈10 s	134

Rakesh M. Shedam – M.Sc, (Ph.D Scholar)

Priyanka P. Kashid.– M.Sc, (Ph.D Scholar)

Shridhar N. Mathad – M.Sc.Ph.D (Head of the Department, Supervisor)

Rahul B. Deshmukh – M.Sc (Assistant Professor)

Mahadev R. Shedam – M.Sc,Ph.D (Head of Department)

Ashok B. Gadkari –M.Sc,Ph.D(Incharge Principal, Supervisor)

- [1] V.D. Kapse, *Preparation of Nanocrystalline Spinel- Type Oxide Materials for Gas Sensing Applications*. Research Journal of Chemical Sciences 5, 7 (2015).
- [2] J. M Smulko, M. Trawka, C. G. Granqvist, R. Ionescu, F. Annanouch, E. Llobet, L. B. Kish, *New Approaches for Improving Selectivity and Sensitivity of Resistive Gas Sensors: A Review*, Sensor Review, 35(4), 340 (2015); <https://doi.org/10.1108/SR-12-2014-0747>.
- [3] G. Sberveglieri (Ed.), *Gas Sensors: principles, Operation and Developments*; Berlin, Germany: Springer Science & Business Media, (2012).
- [4] E. A. Symons, *Catalytic Gas Sensors*. Gas Sensors, 169 (1992); https://doi.org/10.1007/978-94-011-2737-0_5.
- [5] E. Bakker, M. Telting-Diaz, *Electrochemical Sensors*, Analytical Chemistry, 74(12), 2781 (2002); <https://doi.org/10.1021/ac0202278>.
- [6] J. Hodgkinson, R. P. Tatam, *Optical Gas Sensing: A Review*, Measurement Science and Technology, 24(1), 012004 (2012); <https://doi.org/10.1088/0957-0233/24/1/012004>.
- [7] P. Bhattacharyya, *Technological Journey towards Reliable Microheater Development for MEMS Gas Sensors; A Review*, IEEE Transactions on Device and Materials Reliability, 14(2), 589 (2014); <https://doi.org/10.1109/TDMR.2014.2311801>.
- [8] J. D. N. Cheeke, Z. Wang *Acoustic wave gas sensors*, Sensors and Actuators B 59, 146–153, (1999); [https://doi.org/10.1016/S0925-4005\(99\)00212-9](https://doi.org/10.1016/S0925-4005(99)00212-9).
- [9] W. P. Jakubik, *Surface Acoustic Wave-Based Gas Sensors*, Thin Solid Films, 520(3), 986–993, (2011); <https://doi.org/10.1016/j.tsf.2011.04.174>.
- [10] N. Rezlescu, C. Doroftei, E. Rezlescu, P. Lithium Popa, *Ferrite for Gas Sensing Applications*. Sensors and Actuators B: Chemical, 133(2), 420 (2008); <https://doi.org/10.1016/j.snb.2008.02.047>.
- [11] Z. Sun, L. Liu, D. Zeng Jia, W. Pan, *Simple Synthesis of CuFe₂O₄ Nanoparticles as Gas-Sensing Materials*. Sensors & Actuators, B: Chemical, 125(1), 144 (2007); <https://doi.org/10.1016/j.snb.2007.01.050>.
- [12] N. Yamazoe, *New approaches for improving semiconductor gas sensors*. Sensors and Actuators B: Chemical, 5(1–4), 7–19(1991); [https://doi.org/10.1016/0925-4005\(91\)80213-4](https://doi.org/10.1016/0925-4005(91)80213-4).
- [13] A. Chiorino, G. Ghiotti, F. Prinetto, M. C. Carotta, M. Gallana & G. Martinelli, *Characterization of materials for gas sensors. Surface chemistry of SnO₂ and MoO_x-SnO₂ nano-sized powders and electrical responses of the related thick films*, Sensors and Actuators B: Chemical, 59 (2–3), 203 (1999); [https://doi.org/10.1016/S0925-4005\(99\)00221-X](https://doi.org/10.1016/S0925-4005(99)00221-X).
- [14] M. Sugimoto, *The past, present and future of ferrites*, Journal of the American Ceramic Society, 82(2), 269 (1999); <https://doi.org/10.1111/j.1551-2916.1999.tb20058.x>.
- [15] V. R. Singh, *Smart sensors, physics, technology, and applications*, Indian Journal of Pure and Applied Physics 43(1) 7-16 (2005); https://www.researchgate.net/publication/228366667_Smart_sensors_Physics_technology_and_applications#fullTextFileContent.
- [16] D. Bahadur, *Current trends in applications of magnetic ceramic materials* Bulletin of Materials Science, 15 (5), 431 (1992); <http://docplayer.net/104066860-Current-trends-in-applications-of-magnetic-ceramic-materials.html>.
- [17] Z. Tianshu, P. Hing, Z. Jiancheng, K. Lingbing, *Ethanol-sensing characteristics of cadmium ferrite prepared by chemical coprecipitation*, Materials Chemistry and Physics, 61(3), 192 (1999); [https://doi.org/10.1016/S0254-0584\(99\)00133-9](https://doi.org/10.1016/S0254-0584(99)00133-9).
- [18] K. M. Reddy, L. Satyanarayana, S. V. Manorama, R. D. K. Misra, *A comparative study of the gas sensing behavior of nano structured nickel ferrite synthesized by hydrothermal and reverse micelle technique*, Materials Research Bulletin 39(10), 1491 (2004); <https://doi.org/10.1016/j.materresbull.2004.04.022>.
- [19] N. Rezlescu, C. Doroftei, E. Rezlescu, P. D. Popa, *The influence of Sn and MO ion on the structural electrical and gas sensing property of Mg ferrite*, Physica Status Solidi (A) Applications and Materials Science. 203 (2), 306 (2006); <https://doi.org/10.1002/pssa.200521043>.
- [20] G. A. Prinz, *Magneto-electronics*, Science, 282 (5394), 1660–1663. (1998). <https://doi.org/10.1126/science.282.5394.1660>.
- [21] Z. Wang, X. Liu, M. Lv, P. Chai, Y. Liu, J. Meng, *Preparation of ferrite MFe₄O₄ (M= Co, Ni) ribbons with nanoparticles*, Journal of physics chemistry B, 112 (36), 11292 (2008); <https://doi.org/10.1021/jp804178w>.
- [22] E. Manova, B. Kunev, D. Paneva, I. Mitov, L. Petrov, C. Estournès, C.D'Orléan, J. L. Ehspringer, M. Kurmoo, *Mechano-Synthesis, Characterization, and Magnetic Properties of nanoparticles of Cobalt Ferrite, CoFe₂O₄*, Chemistry of Materials 16(26), 5689-5696 (2004); <https://doi.org/10.1021/cm049189u>.

- [23] C. V. G. Reddy, S. V. Manorama, and V. J. Rao, *Semiconducting gas sensor for chlorine based on inverse spinel nickel ferrite*, *Sensors and Actuators B: Chemical*, (55) 1, 90 (Apr. 1999); [https://doi.org/10.1016/S0925-4005\(99\)00112-4](https://doi.org/10.1016/S0925-4005(99)00112-4).
- [24] K. C. Patil, S. S. Manoharan, and D. Gajapathy *Preparation of high density ferrites*, in *Hand Book of Ceramic and Composites*, New York: Marcel Dekker, 1, 469 (2021).
- [25] M. R. Patil, M. K. Rendale, S. N. Mathad, R. B. Pujar, *Structural and IR study of $Ni_{0.5-x}Cd_xZn_{0.5}Fe_2O_4$* *International Journal of Self-Propagating High-Temperature Synthesis*, 24(4) 241 (2015); <https://doi.org/10.3103/S1061386215040081>.
- [26] A. B. Gadkari, T. J. Shinde, P. N. Vasambekar, *Structural and magnetic properties of nanocrystalline Mg–Cd ferrites by oxalate precipitation method*, *Journal of Materials Science: Materials in Electronics*, 21(1) 96(2010); <https://doi.org/10.1016/j.matchar.2009.06.010>.
- [27] Y. Zhihao and Z. Lide, *Synthesis and structural characterization of capped $ZnFe_2O_4$ nanoparticles* *Materials Research Bulletin* 33(11), 1587 (1998). [https://doi.org/10.1016/S0025-5408\(98\)00164-0](https://doi.org/10.1016/S0025-5408(98)00164-0).
- [28] G.R. Dube and V.S. Darshane, *Decomposition of octanol on the spinel system $Ga_{1-x}Fe_xCuMnO_4$* *Journal of Molecular Catalysis* 79(1–3), 285 (Nov. 1993); [https://doi.org/10.1016/0304-5102\(93\)85108-6](https://doi.org/10.1016/0304-5102(93)85108-6).
- [29] S. S. Yattinahalli, S. B. Kapatkar, N. H. Ayachit and S. N. Mathad, *Synthesis and structural characterization of nanosized nickel ferrite*, *International Journal of Self-Propagating High-Temperature Synthesis*, 22(3), 147 (2013); <https://doi.org/10.3103/S1061386213030114>.
- [30] S. A. Wolf, D. D. Awschalam, R. A. Buhrman, J. M. Daughton, S. V. Molnar, M. L. Roukes, A. Y. Chtchelkanova, D. M. Treger, *Spintronics A spin based electronics vision for the future* *Science*, 294 (5546), 1488 (2001); <https://doi.org/10.1126/science.1065389>
- [31] W. Gopel, J. Hesse, J. N. Zemel, *Sensors A Comprehensive Survey* Vol. 9, Wiley-VCH, 1995
- [32] A.B. Gadkari, T.J. Shinde, P.N. Vasambekar, *Influence of rare earth ions on structural and magnetic properties of $CdFe_2O$ ferrites*, *Rare Earth*, 29 (2) 168 (2010); <https://doi.org/10.1007/s12598-010-0029-z>.
- [33] X.Q. Liu, Z. Xu, Y. Liu, Y. Shen, *A novel high performance ethanol gas sensors based on $CdO-Fe_2O_4$ semiconducting materials*, *Sensors and Actuators B: Chemical* 52(3), 270–273 (1998); [https://doi.org/10.1016/S0925-4005\(98\)00278-0](https://doi.org/10.1016/S0925-4005(98)00278-0).
- [34] C. V. G. Reddy, S. V. Manorma, V. J. Rao, *Preparation and characterization of ferrites as gas sensor materials*, *Journal of Materials Science Letters* 19(9) 775 (2000). <https://doi.org/10.1023/a:1006716721984>.
- [35] N. S. Chen, X. J. Yang, E. S. Liu, and J. L. Huang, *Reducing gas-sensing properties of ferrite compounds MFe_2O_4 ($M = Cu, Zn, Cd$ and Mg)*, *Sensors and Actuators B: Chemical* 66(1-3), 178 (2000); [https://doi.org/10.1016/S0925-4005\(00\)00368-3](https://doi.org/10.1016/S0925-4005(00)00368-3).
- [36] Y. Shimiza, S. Kusarao, H. Kuwayama, K. Tanaka, M. Egasira, *Oxygen sensing properties of spinel type oxide, stoichiometric air /fuel combustion control*, *Journal of the American Ceramic Society* 73(4), 818 (1990); <https://doi.org/10.1111/j.1151-2916.1990.tb05120.x>.
- [37] X. Lou, S. Liu, D. Shi, & W. Chu, *Ethanol-sensing characteristics of $CdFe_2O_4$ sensor prepared by sol-gel method*, *Materials Chemistry and Physics*, 105(1), 67 (2007); <https://doi.org/10.1016/J.MATCHEMPHYS.2007.04.038>.
- [38] V. C. B. Pegoretti, P. R. C. Couceiro, C. M. Goncalves, M. D. F. F. Lelis, J. D. Fabris, *Preparation and characterization of tin-doped spinel ferrite*, *Journal of Alloys and Compounds*, 505(1), 125–129(2010); <https://doi.org/10.1016/J.JALLCOM.2010.06.058>.
- [39] H. Suo, F. Wu, Q. Wang, G. Liu, F. Qin, B. Xq, and M. Zhao, *Study on ethanol sensitivity of nanocrystalline $La_{0.7}Sr_{0.3}FeO_3$ based gas sensor*, *Sensors and Actuators B: Chemical*, 45(3), 245(1997); [https://doi.org/10.1016/S0925-4005\(97\)00314-6](https://doi.org/10.1016/S0925-4005(97)00314-6).
- [40] K. Muraishi, N. Hiratsuka, T. Katsube, *Gas sensing characteristics of porous nickel ferrite added with rare earth metal oxides*. *Denki Kagaku oyobi Kogyo Butsuri Kagaku*, 61(7), 907-908 (1993); <https://doi.org/10.5796/electrochemistry.61.907>.
- [41] N. Rezlescu, N. Iftime, E. Rezlescu, C. Doroftei, and P. D. Popa, *Semiconducting gas sensor for acetone based on the fine grained nickel ferrite* *Sensors and Actuators B: Chemical* 114(1) 427 (2006); <https://doi.org/10.1016/j.snb.2005.05.030>.
- [42] S. L. Darshane, R. G. Deshmukh, S. S. Suryavanshi, I. C. Mulla, *Gas sensing properties of zinc ferrite nanoparticles synthesized by the molten salt route*, *Journal of the American Ceramic Society*, 91(8) 2724 (2008); <https://doi.org/10.1111/j.1551-2916.2008.02475.x>.
- [43] S. L. Galagali, R. A. Patil, R. B. Adaki, C. S. Hiremath, S. N. Mathad, A. S. Pujar, R. B. Pujar, *Fourier transform infrared spectroscopy and elastic properties of $Mg_{1-x}Cd_xFe_2O_4$ ferrite systems*. *Journal of Science & Technology* 41 (5), 992-998 (2019); <https://www.thaiscience.info/Journals/Article/SONG/10993099.pdf>.
- [44] R. Vishwaroop, S.N.Mathad, *Synthesis, Structural, W-H plot and Size-Strain analysis of Nano cobalt doped $MgFe_2O_4$ Ferrite*, *Science of Sintering*, 52(3) 349 (2020); <https://doi.org/10.2298/SOS2003349V>.
- [45] R. M. Shedam, A. B. Gadkari, S. N.Mathad, M.R. Shedam *Structural and Mechanical Properties of nano-sized magnesium ferrite by Oxalate Co-Precipitation Method*, *International Journal of Self-Propagating High-Temperature Synthesis*, 26 (1) 75 (2017); <https://doi.org/10.3103/S1061386217010113>.

- [46] S. S. Kakati, T.M.Makandar, M.K. Rendale, S.N Mathad, *Green Synthesis Approach for Nanosized Cobalt Doped Mg–Zn through Citrus Lemon Mediated Sol–Gel Auto Combustion Method*, International Journal of Self-Propagating High-Temperature Synthesis, 31(3), 131 (2022); <https://doi.org/10.3103/S1061386222030049>.
- [47] G. M. Shweta, L. R. Naik, R. B. Pujar, S. N. Mathad, *Cobalt-Doped Nickel Zinc Nanoferrites by Solution-Combustion Synthesis: Structural and Elastic Parameters*, International Journal of Self-Propagating High-Temperature Synthesis 29(3), 157 (2020); <https://doi.org/10.3103/S1061386220030115>.
- [48] P. Rao, R. V. Godbole, S. Bhagwat, *Chlorine gas sensing performance of palladium doped nickel ferrite thin films*, Journal of Magnetism and Magnetic Materials, 405, 219 (2016); <https://doi.org/10.1016/J.JMMM.2015.12.065>
- [49] R. Vishwarup, S. N. Mathad, *Facile synthesis of Nano Mg-Co ferrites ($x = 0.15, 0.20, 0.25, 0.30, 0.35,$ and 0.40) via coprecipitation route: structural characterization*, Materials International, 2(4) 0471 (2020); <https://doi.org/10.33263/Materials24.471476>.
- [50] A. B. Gadkari, T. J. Shinde, P. N. Vasambekar, *Ferrite Gas Sensors*, IEEE Sensors journal, 11(4), 849-861 (2010); <https://doi.org/10.1109/JSEN.2010.2068285>.
- [51] S. Joshi, V.B Kamble, M. Kumar, A. M. Umarji, G. Srivastava, *Nickel Substitution Induced Effects on Gas Sensing Properties of Cobalt Ferrite Nanoparticles*, Journal of Alloys and Compounds 654, 460-466. (2016); <https://doi.org/10.1016/j.jallcom.2015.09.119>.
- [52] A. K. Yadav, R. K. Singh, P. Singh, *Fabrication of Lanthanum Ferrite Based Liquefied Petroleum Gas*, Sensors and Actuators B: Chemical 229, 25 (2016); <https://doi.org/10.1016/j.snb.2016.01.066>.
- [53] X. Yang, S. Zhang, Q. Yu, P. Sun, F. Liu, H. Lu, X. Yan, X. Zhou, X. Liang, Y. Gao, G. Lu, *Solvothermal Synthesis of Porous CuFe_2O_4 Nanospheres for High Performance Acetone*, Sensors and Actuators B: Chemical, 270, 538 (2018); <https://doi.org/10.1016/j.snb.2018.05.078>.
- [54] C. Doroftei, O. S. Prelipceanu, A. Carlescu, L. Leontie, M. Prelipceanu, *Porous Spinel-Type Oxide Semiconductors for High-Performance Acetone Sensors*. In 2018 International Conference on Development and Application Systems (DAS) IEEE 110 (2018). <https://doi.org/10.1109/DAAS.2018.8396081>.
- [55] X. F. Wang, K.M. Sun, S. J. Li, X. Z. Song, L. Cheng, W. Ma, *Porous Javelin-like NiFe_2O_4 Nanorods as n-Propanol Sensor with Ultrahigh-Performance*, Chemistry Select, 3(45), 12871 (2018); <https://doi.org/10.1002/slct.201802879>.
- [56] F. Li, S. Guo, J. Shen, L. Shen, D. Sun, B. Wang, Y. Chen, S. Ruan Xylene, *Gas Sensor Based on Au-Loaded $\text{WO}_3\text{-H}_2\text{O}$ Nano cubes with Enhanced Sensing Performance*. Sensors and Actuators B: Chemical 238, 364 (2017); <https://doi.org/10.1016/j.snb.2016.07.021>.
- [57] X. Yang, H. Li, T. Li, Z. Li, W. Wu, C. Zhou, P. Sun, F. Liu, X. Yan, Y. Gao, et al. *Highly Efficient Ethanol Gas Sensor Based on Hierarchical $\text{SnO}_2/\text{Zn}_2\text{SnO}_4$ Porous Spheres*, Sensors and Actuators B: Chemical, 282, 339 (2019); <https://doi.org/10.1016/j.snb.2018.11.070>.
- [58] Y. H. Choi, D. H. Kim, S. H. Hong, *Gas Sensing Properties of p-Type CuBi_2O_4 Porous Nanoparticulate Thin Film Prepared by Solution Process Based on Metal-Organic Decomposition*, Sensors and Actuators B: Chemical 268, 129 (2018); <https://doi.org/10.1016/j.snb.2018.04.105>.
- [59] Y. Xu, X. Tian, P. Liu, Y. Sun, G. Du, GIn_2O_3 , *Nanoplates with Different Crystallinity and Porosity: Controllable Synthesis and Gas-Sensing Properties Investigation*, Journal of Alloys and Compounds 787, 1063 (2019); <https://doi.org/10.1016/j.jallcom.2019.02.176>.
- [60] T. G. Nenov, S. P. Yordanov, *Ceramic Sensors, Technology and Application*. Lancaster, PA: Technomic, pp. 20 (1996).
- [61] A. Dey, *Semiconductor Metal Oxide Gas Sensors: A Review*, Materials science and Engineering: B 229, 206 (2018); <https://doi.org/10.1016/j.mseb.2017.12.036>.
- [62] N. Rezlescu, E. Rezlescu, F. Tudorache, P.D. Popa, *Gas Sensing Properties of Porous Cu-, Cd-and Zn-Ferrites*. Romanian Reports in Physics 61, (2) 223 (2009); http://rrp.infim.ro/2009_61_2/art05Rezlescu.pdf.
- [63] P. Zhang, H. Qin, W. Lv, H. Zhang, J. Hu, *Gas Sensors Based on Ytterbium Ferrites Nanocrystalline Powders for Detecting Acetone with Low Concentrations*, Sensors and Actuators B: Chemical, 246, 9 (2017); <https://doi.org/10.1016/j.snb.2017.01.096>.
- [64] E. R. Kumar, P. S. P. Reddy; G. S. Devi, S. Sathiyaraj, *Structural, Dielectric and Gas Sensing Behaviour of Mn Substituted Spinel MFe_2O_4 ($M = \text{Zn}, \text{Cu}, \text{Ni}, \text{and Co}$) Ferrite Nanoparticles*, Journal of Magnetism and Magnetic Materials 398, 281 (2016); <https://doi.org/10.1016/j.jmmm.2015.09.018>.
- [65] T. Dippong, E. A. Levei, O. Cadar, *Recent Advances in Synthesis and Applications of MFe_2O_4 ($M = \text{Co}, \text{Cu}, \text{Mn}, \text{Ni}, \text{Zn}$) Nanoparticles*, Nanomaterials 11, 1560 (2021); <https://doi.org/10.3390/nano11061560>.
- [66] A. S. Poghosian, H. V. Abovian, P. B. Avakian, S. H. Mkrtchian, V. M. Haroutunian, *Bismuth Ferrites: New Materials for Semiconductor Gas Sensors*, Sensors and Actuators B: Chemical 4, 545 (1991); [https://doi.org/10.1016/0925-4005\(91\)80167-I](https://doi.org/10.1016/0925-4005(91)80167-I).
- [67] N. Rezlescu, C. Doroftei, P. D. Popa, *Humidity-Sensitive Electrical Resistivity of MgFe_2O_4 and $\text{Mg}_{0.9}\text{Sn}_{0.1}\text{Fe}_2\text{O}_4$ Porous Ceramics*, Romanian Journal of Physics, 52 (3/4), 353 (2007); <https://citeseerx.ist.psu.edu/viewdoc/download?doi=10.1.1.1043.4447&rep=rep1&type>.

- [68] A. Sutka, G. Mezinskas, *Sol-Gel Auto-Combustion Synthesis of Spinel-Type Ferrite Nanomaterials*, *Frontiers of Materials Science* 6, 128 (2012); <https://doi.org/10.1007/s11706-012-0167-3>.
- [69] C. O. Park, S. A. Akber, *Ceramics for chemical sensing*, *Journal Of Materials Science* 38, (23) 4611 (2003); <https://doi.org/10.1023/A:1027402430153>.
- [70] R. S. Morrison, *Selectivity in semiconductor gas sensors*, *Sensors and actuators*, 12, (4), 425 (1987); [https://doi.org/10.1016/0250-6874\(87\)80061-6](https://doi.org/10.1016/0250-6874(87)80061-6).
- [71] G. Zhang, C. Li, F. Cheng, and J. Chen, *ZnFe O tubes: Synthesis and application to gas sensors with high sensitivity and low energy consumption*, *Sensors and Actuators B: Chemical*, 120, (2), 403 (2007); <https://doi.org/10.1016/j.snb.2006.02.034>.
- [72] A. B. Bodade, A. V. Kadu, and G. N. Chaudhari, *Preparation and structural characterization of nano sized BiFe_{0.6} Mn_{0.4} O₃ as a novel material with high sensitivity towards LPG*, *Journal of Sol-Gel Science and Technology*, 45, 27 (2008); <https://doi.org/10.1007/s10971-007-1641-8>.
- [73] B. D. Cullity, *Elements of X-Ray Diffraction*. Reading, MA: Addison Wesley, (1956).
- [74] J. Wu, D. Gao, T. Sun, J. Bi, Y. Zhao, Z. Ning, G. Fan, Z. Xie, *Highly Selective Gas Sensing Properties of Partially Inversed Spinel Zinc Ferrite towards H₂S*, *Sensors & Actuators, B: Chemical*, 235, 258 (2016); <https://doi.org/10.1016/j.snb.2016.05.083>.
- [75] J. Y. Patil, D. Y. Nadargi, J. L. Gurav, I. S. Mulla, S. S. Suryavanshi, *Synthesis of Glycine Combusted NiFe₂O₄ Spinel Ferrite: A Highly Versatile Gas Sensor*, *Materials Letters*, 124, 144 (2014); <https://doi.org/10.1016/j.matlet.2014.03.051>.
- [76] L. Sonali, S. S. Darshane, I. S. Suryavanshi, I. S. Mulla *Nanostructured nickel ferrite: A liquid petroleum gas sensor*, *Ceramics International* 35, 1793 (2009); <https://doi.org/10.1016/j.ceramint.2008.10.013>.
- [77] L. Satyanarayana, K. M. Reddy, and S. V. Manorama, *Synthesis of nano-crystalline Ni_{1-x} Co_x Mn_x Fe_{2-x} O₄ : A material for liquefied petroleum gas sensing*, *Sensors & Actuators, B: Chemical*, 89 (1–2), 62 (2003); [https://doi.org/10.1016/S0925-4005\(02\)00429-X](https://doi.org/10.1016/S0925-4005(02)00429-X).
- [78] L. Satyanarayana, K. M. Reddy, & S. V. Manorama, *Nanosized spinel NiFe₂O₄: A novel material for the detection of liquefied petroleum gas in air*, *Materials Chemistry and Physics*, 82(1), 21–26 (2003); [https://doi.org/10.1016/S0254-0584\(03\)00170-6](https://doi.org/10.1016/S0254-0584(03)00170-6).
- [79] K. M. Reddy, L. Satyanarayana, S. v. Manorama, R. D. K. Misra, *A comparative study of the gas sensing behavior of nanostructured nickel ferrite synthesized by hydrothermal and reverse micelle techniques*. *Materials Research Bulletin*, 39(10), 1491 (2004); <https://doi.org/10.1016/J.MATERRESBULL.2004.04.022>.
- [80] I. Sandu, L. Presmanes, P. Alphonse, P. Tailhades, *Nano structured cobalt manganese ferrite thin films for gas sensor application*, *Thin Solid Films*, 495(1–2) 130 (2006); <https://doi.org/10.1016/j.tsf.2005.08.318>.
- [81] N. Rezlescu, E. Rezlescu, C. L. Seva, F. Tudorache, P. D. Popa, *On the effects of Ga and La ions in MgCu ferrite: Humidity sensitive electrical conduction*, *Crystal Research Technology*, 39(6) 548 (2004); <https://doi.org/10.1002/crat.200310223>.
- [82] E. di Bartolomeo, E. Traversa, M. Baroncini, V. Kotzeva, & R. V. Kumar, *Solid state ceramic gas sensors based on interfacing ionic conductors with semiconducting oxides*, *Journal of the European Ceramic Society*, 20(16), 2691 (2000); [https://doi.org/10.1016/S0955-2219\(00\)00219-3](https://doi.org/10.1016/S0955-2219(00)00219-3).
- [83] A. B. Gadkari, T. J. Shinde, P. N. Vasambekar, *Structural analysis of Y³⁺-doped Mg–Cd ferrites prepared by oxalate co-precipitation method*, *Materials Chemistry and Physics*, 114(2–3), 505 (2009); <https://doi.org/10.1016/J.MATCHEMPHYS.2008.11.011>.
- [84] C. B. Kolekar, P. N. Kamble, A. S. Vaingankar, *X-ray, far IR characterization and susceptibility study of Gd substituted copper cadmium ferrites*, *Indian Journal of Physics* 68(6), 529 (1994); <https://core.ac.uk/download/pdf/158962081.pdf>.
- [85] A. C. F. M. Costa, M. R. Morelli, R. H. G. A. Kiminami, *Microstructure and magnetic properties of Ni–Zn–Sm ferrites*, *Ceramica*, 49, (311) 168 (2003); <https://doi.org/10.1590/S0366-69132003000300011>.
- [86] P. K. Roy, B. B. Nayak, J. Bera, *Study on electro-magnetic properties of La³⁺ substituted Ni–Cu–Zn ferrite synthesized by auto-combustion method*, *Journal of Magnetism and Magnetic Materials*, 320(6), 1128–1132 (2008); <https://doi.org/10.1016/J.JMMM.2007.10.025>.
- [87] X. Fan, H. Ren, Y. Zhang, S. Guo, and X. Wang, *Effect of Nd on microstructure and magnetic properties of Ni–Zn ferrites*, *Rare Metals*, 7(3) 287 (Jun. 2008); [https://doi.org/10.1016/S1001-0521\(08\)60131-X](https://doi.org/10.1016/S1001-0521(08)60131-X).
- [88] Priese, C.; Töpfer, J. *Phase Formation, Microstructure and Permeability of Fe-Deficient Ni-Cu-Zn Ferrites, (I): Effect of Sintering Temperature*. *Magnetochemistry* 2021, 7, 118. <https://doi.org/10.3390/magnetochemistry7080118>
- [89] K. Oura, M. Katayama, A. V. Zotov, V. G. Lifshits, A. A. Saranin, *Elementary Processes at Surfaces I. Adsorption and Desorption*. In: *Surface Science Advanced Texts in Physics*. Springer, Berlin, Heidelberg (2003); https://doi.org/10.1007/978-3-662-05179-5_12.
- [90] M. C. Desjonqueres et al., *Concept in Surface Physics*. Berlin, Germany: Springer-Verlag, <https://doi.org/10.1007/978-3-642-97484-7>.
- [91] L. M. Peng, *New Developments of Electron Diffraction Theory*, *Advances in Imaging and Electron Physics*, 90(C), 205–351 (1994); [https://doi.org/10.1016/S1076-5670\(08\)70085-5](https://doi.org/10.1016/S1076-5670(08)70085-5).

- [92] S. G. Davison and M. Steslicka, *Basic Theory of Surface State*. Oxford, U.K.: Oxford Univ. Press, vol. 3–5, p. 61 (1992).
- [93] Garima Rana, Pooja Dhiman, Amit Kumar, Dai-Viet N. Vo, Gaurav Sharma, Shweta Sharma, Mu. Naushad, Recent advances on nickel nano-ferrite: A review on processing techniques, properties and diverse applications, *Chemical Engineering Research and Design*, Volume 175, 2021, Pages 182-208, ISSN 0263-8762, <https://doi.org/10.1016/j.cherd.2021.08.040>.
- [94] C. O. Park, S. A. Akbar, *Ceramics for chemical sensing*. *Journal of Materials Science* 38, 4611 (2003); <https://doi.org/10.1023/A:1027402430153>.
- [95] K. D. Schierbaum, U. Weimar, W. Göpel, & R. Kowalkowski, *Conductance, work function and catalytic activity of SnO₂-based gas sensors*. *Sensors and Actuators B: Chemical*, 3(3), 205 (1991); [https://doi.org/10.1016/0925-4005\(91\)80007-7](https://doi.org/10.1016/0925-4005(91)80007-7).
- [96] C. Xiangfeng, L. Xingqin, M. Guangyao, *The catalytic effect of SmInO₃ on the gas-sensing properties of CdIn₂O₄*, *Materials Science and Engineering: B*, 64(1), 60 (1999); [https://doi.org/10.1016/S0921-5107\(99\)00144-0](https://doi.org/10.1016/S0921-5107(99)00144-0).
- [97] X. Q. Liu, S. W. Tao, Y. S. Shen, *Preparation and characterization of nanocrystalline α -Fe₂O₃ by a sol-gel process*, *Sensors and Actuators B: Chemical*, 40 (2–3), 161 (1997); [https://doi.org/10.1016/S0925-4005\(97\)80256-0](https://doi.org/10.1016/S0925-4005(97)80256-0).
- [98] M. Sugimoto, *The past, present and future of ferrites*, *Journal of the American Ceramic Society* 82(2), 269 (1999); <https://doi.org/10.1111/j.1551-2916.1999.tb20058.x>.
- [99] S. Tao, F. Gao, X. Liu, & O. T. Sørensen, *Preparation and gas-sensing properties of CuFe₂O₄ at reduced temperature*, *Materials Science and Engineering: B*, 77(2), 172–176 (2000); [https://doi.org/10.1016/S0921-5107\(00\)00473-6](https://doi.org/10.1016/S0921-5107(00)00473-6).
- [100] V. Lantto, P. Romppainen, *Electrical studies on the reactions of CO with different oxygen species on SnO₂ surfaces*. *Surface Science*, 192(1), 243–264 (1987); [https://doi.org/10.1016/S0039-6028\(87\)81174-3](https://doi.org/10.1016/S0039-6028(87)81174-3).
- [101] S. Masti, *Crystallographic, Electrical And Magnetic Properties Of Gd³⁺ Substituted And Non Substituted Mg-Zn Ferrites* *Journal of Engineering, Computers & Applied Sciences (JEC&AS)* 2, (12) (2013).
- [102] N. Rezlescu, E. Rezlescu, F. Tudorache, and P. D. Popa, *Some spinel oxide compounds reducing gas sensors*, *Sensors & Transducers Journal*, 78(4), 1134-1142 (2007); <http://www.sensorsportal.com>.
- [103] G. Martinelli, M. C. Carotta, *Sensitivity to reducing gas as a function of energy barrier in SnO₂ thick-film gas sensor*, *Sensors and Actuators B: Chemical*, 7(1–3), 717 (1992); [https://doi.org/10.1016/0925-4005\(92\)80391-A](https://doi.org/10.1016/0925-4005(92)80391-A).
- [104] K. Arshak, I. Gaidan, *Effects of NiO/TiO₂ addition in ZnFe₂O₄ based gas sensors in the form of polymer thick films*, *Thin Solid Films*, 495(1–2), 292–298 (2006); <https://doi.org/10.1016/j.TSF.2005.08.208>.
- [105] C. Xiangfeng, Z. Chenmou, *Sulfide-sensing characteristics of MFe₂O₄ (M = Zn, Cd, Mg and Cu) thick film prepared by co-precipitation method*, *Sensors and Actuators B: Chemical*, 96(3), 504–508 (2003); [https://doi.org/10.1016/S0925-4005\(03\)00626-9](https://doi.org/10.1016/S0925-4005(03)00626-9).
- [106] L. Bruno, C. Pijolat, R. Lalauze, *Tin dioxide thin-film gas sensor prepared by chemical vapour deposition: Influence of grain size and thickness on the electrical properties*, *Sensors and Actuators B: Chemical*, 18(1–3), 195 (1994); [https://doi.org/10.1016/0925-4005\(94\)87083-7](https://doi.org/10.1016/0925-4005(94)87083-7).
- [107] R. Lalauze, C. Pijolat, S. Vincent, L. Bruno, *High-sensitivity materials for gas detection*, *Sensors and Actuators B: Chemical*, 8(3), 237–243 (1992); [https://doi.org/10.1016/0925-4005\(92\)85024-Q](https://doi.org/10.1016/0925-4005(92)85024-Q).
- [108] J. M. Suh, H. W. Jang, Eom, H. Tae, S. H. Cho, T. & Kim, *Light-activated gas sensing: a perspective of integration with micro-LEDs and plasmonic nanoparticles*, *Materials Advances*, 2, 827-844 (2021); <https://doi.org/10.1039/d0ma00685h>.
- [109] Z. Sun, L. Liu, D. Jia, W. Pan, *Simple synthesis of CuFe₂O₄ nanoparticles as gas sensing materials* *Sensors & Actuators, B: Chemical*, 125(1) 144 (2007); <https://doi.org/10.1016/j.snb.2007.01.050>.
- [110] X. Lou, S. Liu, D. Shi, W. Chu, *Ethanol sensing characteristic of CdFe₂O₄ sensor prepared by Sol-gel*, *Materials Chemistry and Physics*, 105, 66 (2007); <https://doi.org/10.1016/j.matchemphys.2007.04.038>.
- [111] S. Darshane, I. Mulla, *Influence of palladium on gas-sensing performance of magnesium ferrite nanoparticles*. *Materials Chemistry and Physics*, 119(1–2), 319–323 (2010); <https://doi.org/10.1016/J.MATCHEMPHYS.2009.09.004>.
- [112] Y. L. Liu, Z. M. Liu, Y. Yang, H. F. Yang, G. L. Shen, R. Q. Yu, *Simple synthesis of MgFe₂O₄ nanoparticles as gas sensing materials*, *Sensors and Actuators B: Chemical*, 107(2), 600–604 (2005); <https://doi.org/10.1016/J.SNB.2004.11.026>.
- [113] J. Y. Patil, I. S. Mulla, S. S. Suryavanshi, *Gas response properties of citrate gel synthesized nanocrystalline MgFe₂O₄: Effect of sintering temperature*, *Materials Research Bulletin*, 48(2), 778–784 (2013); <https://doi.org/10.1016/J.MATERRESBULL.2012.11.060>.
- [114] Y. Cao, H. Qin, X. Niu, D. Jia, *Simple solid-state chemical synthesis and gas-sensing properties of spinel ferrite materials with different morphologies*, *Ceramics International*, 42(9), 10697 (2016); <https://doi.org/10.1016/J.CERAMINT.2016.03.184>.
- [115] R. K. Kotnala, J. Shah, B. Singh, H. Kishan, S. Singh, S. K. Dhawan, A. Sengupta, *Humidity Response of Li-Substituted Magnesium Ferrite*, *Sensors & Actuators, B: Chemical*, 129, 909 (2008); <https://doi.org/10.1016/j.snb.2007.10.002>.

- [116] Y. Cao, H. Qin, X. Niu, D. Jia, *Simple solid-state chemical synthesis and gas-sensing properties of spinel ferrite materials with different morphologies*, *Ceramics International*, 42(9), 10697–10703 (2016); <https://doi.org/10.1016/J.CERAMINT.2016.03.184>.
- [117] R. K. Kotnala, J. Shah, B. Singh, H. Kishan, S. Singh, S. K. Dhawan, A. Sengupta, *Humidity Response of Li-Substituted Magnesium Ferrite*, *Sensors & Actuators, B: Chemical*, 129, 909 (2008); <https://doi.org/10.1016/j.snb.2007.10.002>.
- [118] N. Rezlescu, N. Iftime, E. Rezlescu, C. Doroftei, P. D. Popa, *Semiconducting gas sensor for acetone based on the fine grained nickel ferrite*, *Sensors & Actuators, B: Chemical*, 114(1) 427 (2006). <https://doi.org/10.1016/j.snb.2005.05.030>.
- [119] A. P. Kazin, M. N. Romyantseva, V. E. Prusakov, I. P. Suzdalev, Y. V. Maksimov, V. K. Imshennik, S. V. Novochikhin, A. M. Gaskov, *Microstructure and Gas-Sensing Properties of Nanocrystalline NiFe₂O₄ Prepared by Spray Pyrolysis*, *Inorganic Materials* 46, 1254 (2010); <https://doi.org/10.1134/S0020168510110178>.
- [120] Y. C. Liang, S. L. Liu, H. Y. Hsia, *Physical Synthesis Methodology and Enhanced Gas Sensing and Photoelectrochemical Performance of 1D Serrated Zinc Oxide–Zinc Ferrite Nanocomposites*, *Nanoscale Research Letters* 10, 1 (2015); <https://doi.org/10.1186/s11671-015-1059-0>.
- [121] M. S. Khandekar, N. L. Tarwal, J. Y. Patil, F. I. Shaikh, I. S. Mulla, S. S. Suryavanshi, *Liquefied Petroleum Gas Sensing Performance of Cerium Doped Copper Ferrite*, *Ceramics International* 39, 5901 (2013); <https://doi.org/10.1016/j.ceramint.2013.01.010>.
- [122] A. B. Gadkari, T. J. Shinde, P. N. Vasambekar, *Ethanol Sensor Based on Nanocrystallite Cadmium Ferrite*, *AIP conference proceedings*, 1665, 050001 (2015); <https://doi.org/10.1063/1.4917642>.
- [123] H. Farahani, R. Wagiran, M. N. Hamidon, *Humidity sensors principle, mechanism, and fabrication technologies: a comprehensive review*, *Sensors*, 14(5), 7881 (2014); <https://doi.org/10.3390/s140507881>.
- [124] Z. Sun, L. Liu, D. zengJia, W. Pan, *Simple synthesis of CuFe₂O₄ nanoparticles as gas-sensing materials* *Sensors and Actuators B: Chemical*, 125 (1) 144(2007); <https://doi.org/10.1016/j.snb.2007.01.050>.
- [125] A. Chapelle, F. Oudrhiri-Hassani, L. Presmanes, A. Barnabe, P. Tailhades, *CO₂ Sensing Properties of Semiconducting Copper Oxide and Spinel Ferrite Nanocomposite Thin Film*. *Applied Surface Science*, 256(14), 4715 (2010); <https://doi.org/10.1016/j.apsusc.2010.02.079>.
- [126] S. Tao, F. Gao, X. Liu, O. T. Sørensen, *Preparation and Gas-Sensing Properties of CuFe₂O₄ at Reduced Temperature*, *Materials Science and Engineering B* 77(2), 172 (2000); [https://doi.org/10.1016/S0921-5107\(00\)00473-6](https://doi.org/10.1016/S0921-5107(00)00473-6).
- [127] E. Fazio, S. Spadaro, C. Corsaro, G. Neri, S. G. Leonardi, F. Neri, N. Lavanya, C. Sekar, N. Donato, G. Neri, *Metal-Oxide Based Nanomaterials: Synthesis, Characterization and Their Applications in Electrical and Electrochemical Sensors* *Sensors*, 21(7), 2494 (2021); <https://doi.org/10.3390/s21072494>.
- [128] L. Yu, S. Cao, Y. Liu, J. Wang, C. Jing, J. Zhang, *Thermal and Structural Analysis on the Nanocrystalline NiCuZn Ferrite Synthesis in Different Atmospheres*, *Journal of magnetism and magnetic Materials*, 301(1), 100-106 (2006); <https://doi.org/10.1016/j.jmmm.2005.06.020>.
- [129] A. C. F. Costa, M. R. Morelli, R. H. Kiminami, *Combustion Synthesis: Effect of Urea on the Reaction and Characteristics of Ni-Zn Ferrite Powders* *Journal of Materials Synthesis and Processing* 9(6), 347 (2001); <https://doi.org/10.1023/A:1016356623401>.
- [130] L. Junliang, Z. Wei, G. Cuijing, Z. Yanwei, *Synthesis and Magnetic Properties of Quasi-Single Domain M-Type Barium Hexaferrite Powders via Sol–Gel Auto-Combustion: Effects of pH and the Ratio of Citric Acid to Metal Ions (CA/M)*, *Journal of Alloys and Compounds*, 479 (1-2), 863 (2009); <https://doi.org/10.1016/j.jallcom.2009.01.081>.
- [131] Y. M. Zhang, Y. T. Lin, J. L. Chen, J. Zhang, Z. Q. Zhu, Q. J. Liu, *A High Sensitivity Gas Sensor for Formaldehyde Based on Silver Doped Lanthanum Ferrite*, *Sensors & Actuators, B: Chemical*, 190, 171 (2014); <https://doi.org/10.1016/j.snb.2013.08.046>.
- [132] S. Singh, A. Singh, R. R. Yadav, P. Tandon, *Growth of Zinc Ferrite Aligned Nanorods for Liquefied Petroleum Gas Sensing*, *Materials Letters*, 131, 31 (2014); <https://doi.org/10.1016/j.matlet.2014.05.167>.
- [133] K. Mukherjee, S. B. Majumder, *Reducing Gas Sensing Behaviour of Nano-Crystalline Magnesium–Zinc Ferrite Powders*, *Talanta*, 81(4-5), 1826-1832 (2010); <https://doi.org/10.1016/j.talanta.2010.03.042>.
- [134] R. P. Patil, P. N. Nikam, S. B. Patil, P. D. Talap, D. R. Patil, P. P. Hankare, *Structural, Magnetic and Gas Sensing Application of Novel Polyol Route Synthesized Cobalt Ferrite*, *Sensor Letters*, 13(9) 785- (2015); <https://doi.org/10.1166/sl.2015.3522>.

Р.М. Шедам^а, П.П. Кашид^а, Ш.Н. Матад^{а*}, Р.Б.Дешмух^б, М.Р. Шедам^с, А.Б. Гадкари^д

Феритові газові сенсори: огляд

^{а*}Кафедра фізики, Технологічний інститут Товариства К.Л.Е, Хублі, Індія, physicsiddu@gmail.com,
physicsiddu@kleit.ac.in;

^бКафедра фізики, Інженерно-технологічний коледж імені Анни Сахеб Данге, Ашта-416301, Індія;

^сКафедра фізики, Новий коледж, Колхатур - 416012, Індія;

^дКафедра фізики, коледж GKG, Колхатур – 416012, Індія

Високочутливі, стабільні та вибірковогазові сенсорикористуються все більшим попитом для виявлення токсичних газів. Для захисту людей, тварин та навколишнього середовищাপотрібно моніторити концентрації цих газів. Металеві ферити (AFe_2O_3 , де А – метал) є основним фактором у цьому напрямку. За останнє десятиліття розробка сенсорів феритових газів досягла значних успіхів у виявленні токсичних газів із вихлопних газів транспортних засобів, біологічних небезпек, моніторингу навколишнього середовища та моніторингу забруднення. Для сенсорів феритового газу важливо враховувати такі параметри, як фазоутворення, розмір кристалітів, розмір частинок, розмір зерна, легуючі домішки, площа поверхні, чутливість, селективність, робоча температура, концентрація газу, час відгуку та час відновлення. Існують різні матеріали для виявлення різних газів, як чадний газ (CO), вуглекислий газ (CO₂), метан (CH₄), етиловий спирт (C₂H₅OH), сірководень (H₂S), C₂H₅COOH, кисень (O₂), водень (H₂), хлор (Cl₂), NH₃, C₄H₁₀, CH₃COOH, бензин, ацетилен, бензин і скраплений нафтовий газ (LPG). Для виготовлення сенсорів феритового газу використовуються різні методи. Крім того, наведено короткий опис різних методів, які використовуються для синтезу сенсорів феритового газу. Викладено низку міркувань щодо конструкції феритових сенсорів газу, включаючи температуру прожарювання, робочу температуру, концентрацію допantu та умови оптимізації. Стаття містить комплексний огляд феритів як газових сенсорів, таких як нікель, мідь, цинк, кадмій, кобальт, магній, марганець та багатокомпонентних феритів, виготовлених різними методами. Здійснено комплексний огляд феритів як газових сенсорів, таких як нікель, мідь, цинк, кадмій, кобальт, магній, марганець, а також багатокомпонентних феритів, виготовлених різними методами.

Ключові слова: газові сенсори, феритові товсті плівки.